Modeling of light transmittance measurement in a finite layer of whole blood – a collimated transmittance problem in Monte Carlo simulation and diffusion model

Janusz MROCZKA, Remigiusz SZCZEPANOWSKI

Chair of Electronic and Photonic Metrology, Wrocław University of Technology,
ul. Bolesława Prusa 53/55, 50-317 Wrocław, Poland; e-mail: janusz.mroczka@pwr.wroc.pl

The paper presents the modeling of transmittance measurement in a finite layer of whole blood. To describe light propagation in whole blood medium, a Monte Carlo simulation was used. The propagation of light in whole blood medium in the model required the assumption of photon transport approximation in highly scattering media. We have analyzed collimated-diffuse transmittance, which depended on the technique of free path length simulation. The Monte Carlo simulation was compared with the diffusion model designed for a finite incident light beam and available measurement data of whole blood optical density. The research revealed that discrepancy between the models discussed may be attributed to inaccuracy of the diffusion model due to an increase of anisotropic radiance under the thin sample conditions. Moreover, comparison of the Monte Carlo simulation versus measurement data showed that adding off-sets enabled agreement between them for hematocrit up to 60–70%, which is sufficient for many applications in oximetry. In fact, discrepancy in the Monte Carlo simulation, requiring off-sets to fit measurement data, most likely originates from measurement problem, such as divergence of light source or perturbation of light beam.

Keywords: multiple light scattering, Monte Carlo simulation, diffusion model, whole blood.

1. Introduction

The non-invasive, optical measurement methods are commonly used in diagnosis of whole blood [1–3]. In this respect, one may consider a reflectance method taking into account the backscattered light from object, and a transmission method, which concerns the scattered light travelling through a finite layer of whole blood [1, 2]. Measuring scattered light enables us to estimate the elementary hematological parameters of whole blood, such as hematocrit and oxyhemoglobin saturation [2, 3]. Thus, a theoretical model of light propagation in blood medium, which defines a dependence between the hematological parameters of whole blood and the measurement quantities, is needed.

The important fact is that when modeling the light propagation in whole blood it is necessary to consider the multiple light scattering phenomenon [3]. The first model describing this phenomenon in whole blood was developed by TVERSKY [4]. However, it was designed for a very simplified measuring system and considered the multiple scattering for a plane only [4]. The experimental validation of this model showed that it can only be used for a very thin layer of whole blood [5]. Another theoretical approach which allows us to predict multiple light scattering in a whole blood sample is diffusion model [2, 3]. According to the diffusion theory, light propagation is considered to be a change of photon flux travelling in the whole blood medium due to both scattering and absorption by the erythrocytes. Hence, such a theoretical approach helps to describe spatial distribution of scattered light in the medium. This model appeared to be useful in more complex optical geometry, which has contributed to the fast development of new constructions for reflectance and transmission oximeters [1, 2].

There are some limitations of diffusion theory in the biological tissue applications. Because of the boundary conditions required to solve the diffusion equation, which is a special case of the general transport equation, the application of diffusion model is restricted in the region close to the light source and to interface boundaries [6–8]. Moreover, in the above-mentioned conditions, there may occur differences between the model and measurement data caused by strong scattering properties of media [7, 9, 10] such as whole blood. The scattering properties of whole blood medium depends on size, shape and concentrations of erythrocytes in a sample, and are given by the scattering coefficient

$$\mu_s = \frac{H\sigma_s(1-H)(1.4-H)}{V_0} \tag{1}$$

where V_0 is the volume of the erythrocyte, H is the hematocrit of whole blood, and σ_s is the scattering cross-section of single erythrocytes [2]. The absorption coefficient μ_a, which takes into account the oxyhemoglobin saturation of whole blood (SaO_2), determines macroscopic ability of whole blood to absorb light and is given by

$$\mu_a = \frac{H\left[\sigma_{ao}SaO_2 + \sigma_{ar}(1-SaO_2)\right]}{V_0} \tag{2}$$

where σ_{ar} is the absorption cross-section of the erythrocyte with fully deoxygenated hemoglobin and σ_{ao} is the cross-section of the erythrocyte with fully oxygenated hemoglobin [2]. A very high albedo coefficient of whole blood ($a = \mu_s/(\mu_s + \mu_a) > 0.99$) points out that whole blood should also be considered as a highly scattering medium. Single erythrocytes in such a medium are primary scatterers. The angular distribution of scattered light around this scatterer can be estimated by an asymmetry factor g, *i.e.*, the mean value of the cosine of scattering angle for an isolated scatterer. When the

scattering by a particle is isotropic, $g = 0$, and it it is entirely in the forward direction, then $g = 1$. The light is very strongly scattered by erythrocyte in a forward direction ($g > 0.9$) and its phase function is forward-peaked. Because of the domination of scattering over absorption, in the modeling of light propagation in highly scattering media one should consider the assumption of the photon transport approximation, which means that solution of the integro-differential diffusion equation is not available under all conditions, relevant for biological media [8]. For uniform radiation and predominant scattering, the photon transport approximation requires isotropic transport scattering coefficient $\mu'_s = \mu_s(1 - g)$ instead of coefficient μ_s.

Contrary to the diffusion theory, the Monte Carlo simulation can consider phenomena observed during light propagation close to the light source and the interface boundaries of optical geometry without simplifying its structure. That is why, this particular model can be used to simulate the measurements of light propagation in tissue, which requires more sophisticated measuring equipment [6–9]. However, in the case of highly scattering media, including biological tissue, the numerical simulation of photon transport using Monte Carlo simulation is ineffective, because of a very high computational cost, *i.e.*, many histories of photons are required to obtain precise results and this may be time-consuming [7, 11]. Consequently, the numerical simulation of the light propagation for highly scattering media requires an assumption of photon transport approximation, which leads to satisfactory accuracy of the Monte Carlo model with measurement data [6]. However, a disagreement between the Monte Carlo simulation and the diffusion model or Kubelka–Munk model was noticed in evaluation of transmittance at small optical path [6, 7, 12].

Since whole blood is a highly scattering medium, the Monte Carlo simulation requires also the assumption of photon transport approximation [12, 13]. A contentious issue is the modeling of collimated transmittance measurement in a flow-through cuvette, whose sample depth insignificantly differs from the transport mean free path length ($L = [\mu_s(1 - g) + \mu_a]^{-1}$). In such conditions a component of collimated transmittance in diffusion model for a finite layer had to be corrected. This indicates the existence of additional mechanism, where the light beam travels nearby the source of light [2]. In general, the transmittance in Monte Carlo model depends on the number of photon collisions in medium. The collimated transmittance, especially, refers to the photons which undergo one or no collision at all [14]. Finally, to describe the light propagation in whole blood we have proposed a new model, where the simulation flow depends strictly on the number of photon collisions in medium, which distinguishes between two methods of free path length calculation. This means that the light flux incident on whole blood sample in a collimated form travels through a finite layer of whole blood, and abandons it as a diffuse light flux. Additionally, we specified the optical properties of whole blood, such as index of refraction, and values of optical coefficients using the T-matrix method, assuming that erythrocytes are modeled as an ensemble of randomly oriented oblate spheroids [15]. Our predictions of Monte Carlo simulation have been compared with the diffusion model for a finite whole blood sample and available transmittance measurement data of whole blood [2].

2. Diffusion model

In highly scattering media the multiple scattering causes fast loss of coherence of travelling light wave in medium, consequently the polarization of light wave in such a medium can be neglected [3]. In this case the transmitted light flux is described as a transport of single photons, which undergo both absorption and elastic scattering while passing through the medium [2, 7, 8]. The change of propagating light flux in medium is described by the diffusion equation that is the approximation of the Boltzman stationary transport equation

$$\nabla^2 \psi(\hat{\rho}) - \frac{\mu_a}{D} \psi(\hat{\rho}) = -\frac{1}{D}\Big[S_0(\hat{\rho}) - 3D\nabla \cdot S_1(\hat{\rho})\Big] \tag{3}$$

where ψ is the diffuse light flux, $S_0(\hat{\rho})$ and $S_1(\hat{\rho})$ are the first two terms in the Legendre polynomial expansion of the source function at any point of medium $\hat{\rho}$, D is the modified diffusion constant, $D = 1/[3(\mu_s' + \mu_a)]$. The diffuse light flux $\psi(\hat{\rho})$ is defined as the total amount of diffuse light power that passes through a small sphere located at the (z, r) divided by the cross-sectional area of that sphere [8].

Figure 1 shows the optical geometry for the transmittance measurement used in the diffusion model. The collimated, monochromatic source of light with the circular aperture of radius a produces the light flux, which falls upon the sample surface of thickness z_0 normally. The circular detector of radius b is coaxial with the radiation source. In the diffusion model a whole blood sample is assumed to extend along x and y axes infinitely. For the light flux travelling close to the interface boundaries of whole blood slab at $z = z_0$ and $z = 0$, the following boundary conditions are derived by Reynolds *et al.* [1] for a finite incident light beam
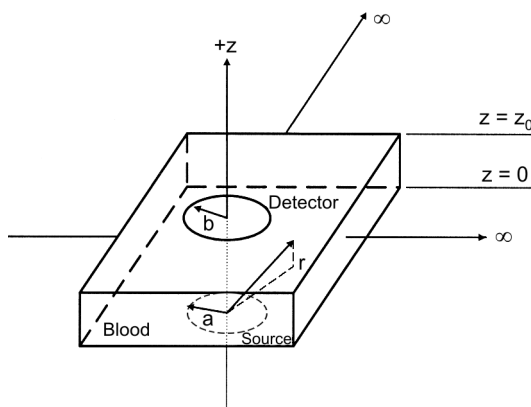
Fig. 1. Optical geometry in diffusion model [2]. Circular source with radius a emits collimated light flux, which is incident normally upon whole blood slab of thickness z_0. Circular detector with radius b is coaxial with source of radius a.

$$\psi(\hat{\rho}) + \frac{3KD\partial\psi(\hat{\rho})}{\partial z} = 0 \qquad (z = z_0),$$

$$\psi(\hat{\rho}) - \frac{3KD\partial\psi(\hat{\rho})}{\partial z} = 0 \qquad (z = 0)$$

(4)

where K is the extrapolation distance of Miln's asymptotic flux ($K = 0.7104$) [2, 3, 16]. In the measurement system shown in Fig. 1, the total transmittance received over the detector surface is given by

$$T_{\text{tot}} = T_{\text{diff}} + T_{\text{c}}$$

(5)

where the component T_{c} is the collimated transmittance, and T_{diff} − the diffuse transmittance. The diffuse transmittance T_{diff} is defined as a ratio of intensity $I(b)$ received by the circular surface of detector to the intensity of light emitted from the source $I(a)$

$$T_{\text{diff}} = \frac{I(b)}{I(a)}.$$

(6)

The intensity $I(b)$ depends on the mutual relation between the radius of detector and the radius of source, and is given by

$$I(b) = \sum_{n=1}^{\infty} -\frac{\psi_0 \mu'_s}{N_n \lambda_n \left(k_n^2 + \mu_t^2\right)} z_n k_n \cos\left(k_n z_0 + \gamma_n\right)$$

$$\times \begin{cases} \dfrac{a^2}{2} - ba I_1(\lambda_n a) K_1(\lambda_n b), & a < b, \\[2mm] \dfrac{b^2}{2} - ba I_1(\lambda_n b) K_1(\lambda_n a), & a > b \end{cases}$$

(7)

where I_1 and K_1 are the first-order modified Bessel functions of the first and second kind, z_n and λ_n are appropriate sequences of numbers, N_n is the eigenvalue normalization constant, k_n are the eigenvalues, and γ_n is the phase function [2]. The diffuse transmittance T_{diff} received by the detector is given by

$$T_{\text{diff}} = I(b)\left[\int_0^a \psi_0 r \,\mathrm{d}r\right]^{-1} = \frac{2I(b)}{\psi_0 a^2}.$$

(8)

The component of the collimated transmittance T_c of Eq. (3) has the following form:

$$T_c = \exp(-\mu_t d) \tag{9}$$

where $d = z_0$ is the sample depth of a rectangular flow-through cuvette, μ_t is the extinction coefficient, describing the influence of both scattering and absorption on the attenuation of the travelling light flux in medium, and it equals $\mu_t = \mu_s + \mu_a$. Nevertheless, the collimated transmittance had to be experimentally validated, because the transport coefficient μ'_s caused significant discrepancy compared to the measurement results. The same problem with appropriate definition of the collimated transmittance was mentioned in [17].

3. Monte Carlo simulation in whole blood

3.1. Path of photon

In the Monte Carlo simulation a photon transport is treated as a Markov chain, where states are successive photon collisions with the particles of the medium [18]. When the photon flux is travelling through the whole blood medium, it is necessary to estimate the appropriate probability density for the events of photons occuring. If the extinction coefficient μ_t is constant, the probability of photon absorption amounts to $p = \mu_a/\mu_t$, whereas the probability of scattering in the medium is given by $q = \mu_s/\mu_t$. The free path length of photon l depends on the extinction coefficient μ_t, and can be obtained with a high accuracy as follows:

$$l = -\frac{\ln \alpha}{\mu_t} \tag{10}$$

where α is the uniformly distributed random number over the interval [0..1] [18, 19] The values of number α are obtained using the pseudo-random generator [19, 20]. The trajectory of a photon moving in the medium is specified by the equation

$$\hat{r}' = \hat{r} + \hat{\omega} \cdot l \tag{11}$$

where $\hat{r}$ is the position vector of photon, $\hat{\omega}$ the unit vector of photon direction, l is the free path length of photon, and $\hat{r}'$ is the position vector of photon after each of its collisions [18].

3.2. Numerical simulation of scattering

In highly scattering media the light scattering at any angle can be approximated using Henyey–Greenstein phase function [7, 19, 21]. After each photon collision a simulation of a new scattering angle θ is calculated using the following expressions:

$$\cos\theta = \begin{cases} \dfrac{1}{2g}\left[1+g^2-\left(\dfrac{1-g^2}{1-g+2g\alpha}\right)^2\right] & \text{if} \quad g \neq 0, \\[2em] 2\alpha-1 & \text{if} \quad g = 0 \end{cases} \qquad (12)$$

where g is the asymmetry factor of erythrocyte, and α is a random number [19, 21]. If a photon is scattered at the angle (θ, φ), a new direction (ω'_x, ω'_y, ω'_z) after its collision is specified by [18, 19]

$$\omega'_x = \frac{\sin\theta}{\sqrt{1-\omega_z^2}}(\omega_x\omega_y\cos\varphi - \omega_y\sin\varphi) + \omega_x\cos\theta,$$

$$\omega'_y = \frac{\sin\theta}{\sqrt{1-\omega_z^2}}(\omega_y\omega_z\cos\varphi + \omega_x\sin\varphi) + \omega_y\cos\theta, \qquad (13)$$

$$\omega'_z = -\sin\theta\cos\varphi\sqrt{1-\omega_z^2} + \omega_z\cos\theta.$$

When the direction of photon propagation is getting close to normal to the slab surface (parallel to the z-axis in measuring system) so that $|\omega_z| > 0.99999$, a new direction of photon propagation is specified by

$$\omega'_x = \sin\theta\cos\varphi,$$

$$\omega'_y = \sin\theta\sin\varphi, \qquad (14)$$

$$\omega'_z = \frac{\omega_z}{|\omega_z|}\cos\theta.$$

The isotropic, azimuthal angle φ is simulated using a more effective rejection method, where [18]

$$\cos\varphi = \frac{1-2\alpha_1}{\sqrt{(1-2\alpha_1)^2 + (1-2\alpha_2)^2}},$$

$$\qquad (15)$$

$$\sin\varphi = \frac{1-2\alpha_2}{\sqrt{(1-2\alpha_1)^2 + (1-2\alpha_2)^2}}$$

with the following condition being satisfied $W = (1 - 2\alpha_1)^2 + (1 - 2\alpha_2)^2 \leq 1$, and α_1, α_2 are the independent random numbers in the interval of [0..1]. If W is greater than one, α_1, α_2 are drawn again.

3.3. Definition of transmittance

The transmittance of light in the model depends on the way the free path photon is simulated. Before the first collision of photon the simulation of free path length l is carried out using Eq. (10), which suits the collimated component T_c in the diffusion model. If photons do not reach the detector after the first collision, the diffuse part of light is simulated using the approximation of the photon transport derived by Miln [3, 7, 16, 18]. Hence, the absorption of photon is calculated using the probability of so-called transport albedo a' survival, and further location of moving photons is specified by the effective mean free path length l'

$$a' = \frac{\mu_s(1 - g)}{\mu_s(1 - g) + \mu_a},$$

$$l' = \frac{\ln \alpha}{\mu_s(1 - g) + \mu_a}.$$

(16)

So, we deal with the simulation of the collimated-diffuse transmittance. Eventually, after numerical analysis of all trajectories of each photon, the total transmittance for the sample of whole blood will be determined.

3.4. Optical geometry

In general, the Monte Carlo method allows no restriction concerning the optical geometry of measuring system. It is possible to implement a simple optical geometry for the transmittance measurement or a more complex measuring system, such as the double sphere of Ulbricht for reflectance measurement [12, 13]. The optical geometry for the transmittance measurements used in our Monte Carlo model is shown in Fig. 1. We have assumed that the source of light is the Ne-He laser or light-emitting diode (LED), producing collimated, monochromatic light beam.

4. Optical properties of whole blood

The primary scatterers in whole blood are erythrocytes considered to be homogenous particles, larger than the incident wavelength [3, 22]. The whole blood suspension is made of the erythrocytes placed in medium with a given osmolality [23, 24]. Under such medium conditions erythrocytes are prevented from undesirable deformability, volume increase, spherocitosis, or hemolysis [24]. Usually, the measurements of light transmittance in whole blood are performed in saline, *i.e.*, mostly 0.9% water solution of NaCl, isotonic relative to plasma where its osmolality equals 300 mOsm, ensuring

the maintenance of normal conditions in organism [25]. With the above-mentioned osmolality the single erythrocytes can be modeled as oblate spheroids with a volume of about 90 μm^3 and the axial ratio $\xi = 3.28$ [26]. The content of hemoglobin in a single erythrocyte is about 95% of the cell volume, therefore the real part of refraction index n of erythrocyte depends on the hemoglobin concentration HC

$$n = n_0 + \alpha\,\text{HC} \qquad (17)$$

where n_0 is the refraction index for erythrocyte without hemoglobin, α is the specific refraction increment [22]. The absorption properties of blood hemoglobin are determined by the imaginary part of the refraction index

$$k = \frac{\ln 10}{\pi M}\,\lambda\,\varepsilon_{\mu M}\,\text{HC} \qquad (18)$$

where M is the molecular weight of hemoglobin (66500 g/mol), λ is the incident wavelength, $\varepsilon_{\mu M}$ is the molar extinction coefficient of hemoglobin dependent on wavelength λ, expressed in $cm^2/\mu mol$ [22].

It is necessary to consider whole blood as an ensemble of randomly oriented oblate spheroids suspended in saline. To compute the optical properties of such erythrocytes the T-matrix method was chosen [15, 27]. In this case, the average cross-sections of erythrocytes σ and average asymmetry parameter g over the size distribution of particles had to be calculated. For estimating the influence of the erythrocyte shape on the light scattering by a single particle, one should also calculate the optical properties for spherical erythrocytes with volume equivalent to spheroidal scatterers (assuming the axial ratio $\xi = 1.0$ for T-matrix computation [27]). The values of optical parameters

T a b l e 1. Optical parameters for erythrocyte – T-matrix method.

	ξ	λ [nm]	σ_s [μm^2]	σ_{ao} [μm^2]	g	a' [*]	L [mm] [*]
100% oxygen saturation	1	632.8	58.11	0.1167	0.99193	0.677	0.553
		660	55.67	0.0495	0.99163	0.831	0.683
		813	41.87	0.0824	0.98963	0.734	0.647
	3.28	632.8	50.63	0.1168	0.98959	0.703	0.510
		660	48.19	0.0497	0.98910	0.847	0.617
		813	36.29	0.0823	0.98660	0.755	0.597
0% oxygen saturation	1	632.8	58.08	0.3580	0.99193	0.415	0.327
		660	55.42	0.2405	0.99164	0.502	0.414
		813	41.85	0.1059	0.98963	0.682	0.603
	3.28	632.8	50.37	0.3580	0.98953	0.435	0.316
		660	47.99	0.2405	0.98913	0.531	0.390
		813	36.27	0.1058	0.98661	0.706	0.556

*Transport albedo and transport mean free path for a typical level of hematocrit (45%).

computed for equal-volume erythrocyte with their different shapes are presented in Tab. 1. The calculations were performed at the standard wavelengths of interest in whole blood oximetry (in the red and infrared range), the selection of which was conducted according to the properties of hemoglobin [1, 2, 28, 29].

The volume of a single erythrocyte was 90 μm^3, the refraction index of saline [23] $N = 1.336$, and hemoglobin concentration in erythrocyte [22] HC = 34 g/dL, respectively. The values of coefficients α and n_0 in wavelength range 500–1200 nm were constant [22]: $\alpha = 0.001942$ dL/g and $n_0 = 1.335$.

The values of cross-sections for the erythrocytes modeled as oblate spheroid particles are insignificantly smaller than the ones for the spherical particles. It can be seen that distribution of scattered light around the spheroidal erythrocyte is less forward-peaked and the ability to attenuate the light is smaller than in the case of spherical particles with the equivalent volume.

5. Transmittance simulation in finite layer of whole blood: Monte Carlo simulation versus diffusion model

We have compared the predictions based on the Monte Carlo simulation with the diffusion model of Steinke and Shepherd [2] designed for a finite diameter of incident light beam. The simulations for both models have been carried out in the optical geometry (Fig. 1). In the Monte Carlo simulation it has been assumed that dimensions of the whole blood slab along the x, y axes are larger than optical paths of the flow-through cuvette d. We have implemented both mathematical models in MATLAB. Since photon trajectories in Monte Carlo model were simulated on the basis of absorption, the number of photons emitted from light source reached up to 100 000. This ensured high accuracy and repeatability of results. Theoretically, Monte Carlo solutions can be obtained for any desired accuracy, because it is proportional to $1/\sqrt{N}$, where N is the number of photons propagated [10, 20] For the maximum number of emitted photons, the relative error is less than one percent. At longer optical paths in the case of non-oxygenated whole blood some irregularities had been found in Monte Carlo simulation, caused by stronger attenuation of light flux due to absorption. The high accuracy, however, will require the propagation of a larger number of photons and consequently enormous amounts of computation time.

To compare both models, we have simulated the curves of the optical density (OD) as a function of hematocrit and also oxyhemoglobin saturation at the fixed optical path. The optical density of whole blood was based on the total transmittance OD = $-\log(T_{tot})$. The curves of whole blood optical density versus hematocrit shown in Figs. 2, 3 were compared for completely oxygenated and deoxygenated whole blood suspensions. The light source was the Ne-He laser (632.8 nm) with a distance from the detector of 1.0, 1.5, and 2.0 mm, respectively, consistent with the optical depths of typical cuvette for the whole blood measurement. Using the light source with small divergence beam offered the possibility of simulating the conditions where the whole incident light beam was fully received by the light detector.
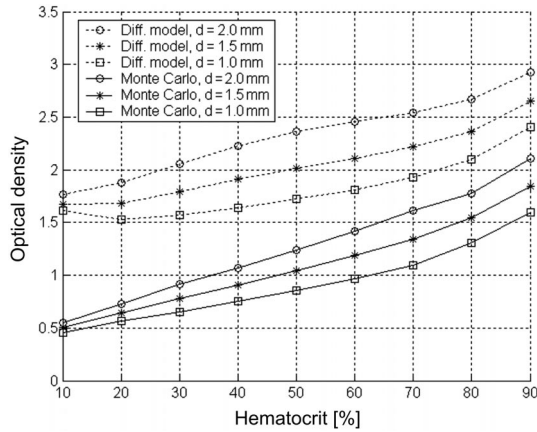
Fig. 2. Comparison of Monte Carlo simulation and diffusion model. Optical density of whole blood *vs.* hematocrit for completely oxygenated hemoglobin, at sample depth: 1, 1.5, 2 mm. The wavelength is 632.8 nm, source radius $a = 0.685$ mm, detector radius $b = 1.0$ mm.
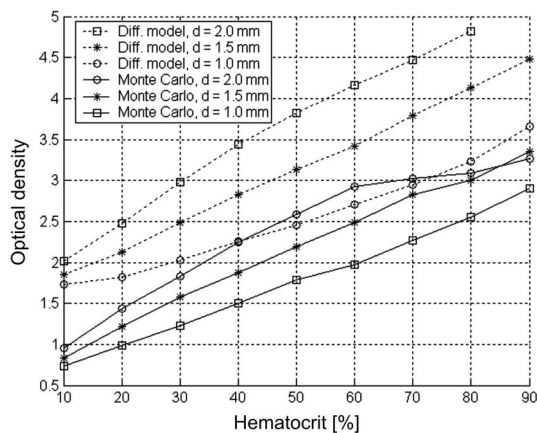
Fig. 3. Comparison of Monte Carlo simulation and diffusion model. Optical density of whole blood *vs.* hematocrit for completely deoxygenated hemoglobin at sample depth of 1, 1.5, 2.0 mm. The wavelength is 632.8 nm, source radius $a = 0.685$ mm and detector radius $b = 1.0$ mm.

Although the shape of the optical curves is similar, the predictions of Monte Carlo simulation differ from the diffusion model by an off-set, as shown in Figs. 2 and 3. The source of the discrepancy between the models derives from the small length of optical paths compared with transport mean path length for whole blood. As was shown by Flock, a stable and isotropic pattern of radiance in biological tissue might be expected at a depth greater than 10 times the transport mean free path [7]. When the lengths of optical paths are close to the transport mean path length (see Tab. 1), the influence of the anisotropic radiance on the light propagation predicted by the diffusion model is observed. Therefore, the high values of asymmetry parameter
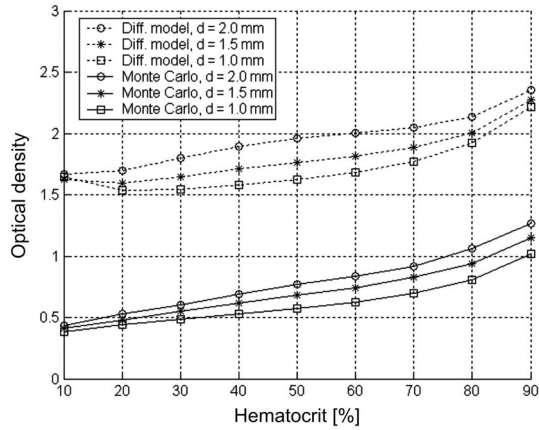
Fig. 4. Comparison of Monte Carlo simulation with diffusion model. Optical density of whole blood *vs.* hematocrit for completely oxygenated hemoglobin, at sample depth: 1, 1.5, 2 mm. The wavelength is 660 nm, the radius of source $a = 2.0$ mm and the radius of detector $b = 1.5$ mm.
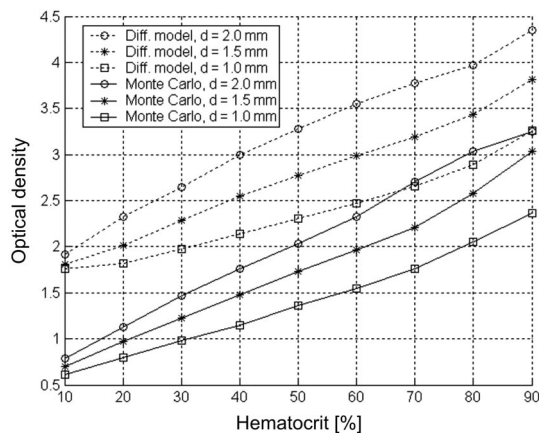
Fig. 5. Comparison of Monte Carlo simulation and diffusion model. Optical density of whole blood as a function hematocrit for completely deoxygenated hemoglobin, at sample depth: 1, 1.5, 2 mm. The wavelength is 660 nm, the radius of source $a = 2.0$ mm and the radius of detector $b = 1.5$ mm.

($g \rightarrow 1$) and the low values of transport albedo (when $a' < 0.8$ according to reference [7]) produce angular radiance distribution less consistent with the linear anisotropy assumed in deriving the diffusion equation [7, 10]. Thus, the diffusion model is getting more inaccurate than Monte Carlo simulation in a thin layer of sample due to an increase of anisotropic radiance in the medium. The major advantage of Monte Carlo simulation under those conditions is its ability to examine in detail the behaviour of the radiance through analysis of each photon. Similar results were obtained for wavelength 660 nm (Figs. 4, 5), where the aperture of the circular source is smaller than the aperture of detector in the optical geometry.
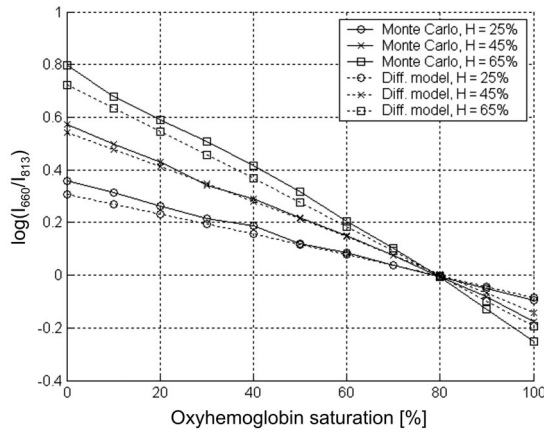
Fig. 6. Relative transmittance $\log(I_{660}/I_{813})$ as a function of the oxyhemoglobin saturation. Monte Carlo simulation *vs.* diffusion model. Radius of source $a = 2.0$ mm, radius of detector $b = 1.5$ mm. The sample depth of flow-through cuvette is 1.27 mm.
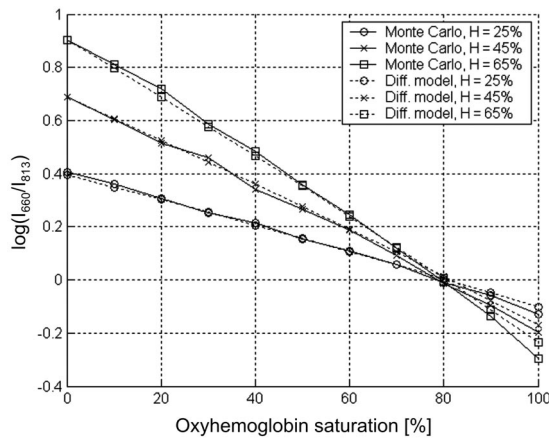
Fig. 7. Relative transmittance $\log(I_{660}/I_{813})$ as a function of oxyhemoglobin saturation. Monte Carlo simulation *vs.* diffusion model. Radius of source $a = 2.0$ mm, radius of detector $b = 1.5$ mm. The sample depth in flow-through cuvette is 1.6 mm.

Subsequently, we have simulated the dual-wavelength transmittance measurement as a function of oxyhemoglobin saturation (typical wavelengths: 660 and 813 nm). The selection of 660 nm wavelength in the oximetry enables the measurement of optical density with linear changes of whole blood extinction coefficients as a function of oxygen saturation [28, 29]. The use of LED of 813 nm wavelength enables measurements near the isobestic point for hemoglobin, when absorption and scattering coefficients of hemoglobin do not depend on oxygen saturation [2, 28, 29]. The simultaneous measurement of light intensity at two different wavelengths allows us to avoid problematic measurement of light source, especially LEDs with significant

divergence [2]. The research was carried out in a flow-through cuvette geometry with thickness 1.27 and 1.6 mm. The curves of relative transmittance $\log(I_{660}/I_{813})$ are presented in Figs. 6 and 7. The characteristics of the relative transmittance shown in Figs. 6, 7, have, as expected, a similar course and a linear character. Nevertheless, the relative transmittance predicted by the Monte Carlo simulation at the lower level of the oxyhemoglobin saturation is insignificantly higher than results of the diffusion model. This discrepancy is observed at the shorter optical path, when the transport albedo becomes lower and inaccuracy of diffusion model increases.

6. Experimental validation of Monte Carlo simulation in whole blood

To validate the usefulness of Monte Carlo simulation, the measurement data of the optical density of whole blood were used, see Tab. 2.

The cross-sections of erythrocytes used for the validation of Steinke and Shepherd diffusion model [2] were calculated for erythrocytes modeled as spheres using the Lorenz–Mie theory. Nevertheless, they found that the values of asymmetry factor g, computed by the Lorenz–Mie theory, were inappropriate during the validation of diffusion model. Thus, only the asymmetry parameter g obtained from the goniometric data enabled a proper comparison of the diffusion model with the measurement, which indicated that a more complex shape of particle was needed to approximate cells. It is difficult to compare the cross-sections presented in Tab. 2 with the T-matrix computation, in regard of the lack of specified whole blood refraction indices in Steinke and Shepherd measurement. However, the lower asymmetry parameters g computed for the randomly oriented spheroids seem to be closer to the goniometric parameters than values of the spherical particles.

The whole blood measurements of Steinke and Shepherd have been carried out in flow through cuvette geometry of sample depth 1.27 and 1.6 mm. In Figure 8, the measurement data of optical density as a function of hematocrit are compared with the predictions of models at the Ne-He laser wavelength. Using the laser Ne-He ensures

T a b l e 2. Optical parameters of erythrocyte specified by STEINKE and SHEPHERD [2].

λ [nm]	σ_s [μm^2]	σ_{ao} [μm^2]	σ_{ar} [μm^2]	g	$L^{a)}$ [mm]	$a'^{a)}$	$L^{b)}$ [mm]	$a'^{b)}$
632.8	63.72	0.155	0.473	0.9845	0.298	0.769	0.202	0.522
660	60.65	0.0656	0.318	0.984	0.349	0.885	0.242	0.615
800	45.59	0.1186	0.1462	0.980	0.336	0.801	0.321	0.765
813	45.59	0.1092	0.1404	0.980	0.342	0.814	0.324	0.773

[a)] Transport albedo and transport mean free path for typical level of hematocrit (45%), the case of oxygenated whole blood.

[b)] Transport albedo and transport mean free path, the case of fully non-oxygenated whole blood (hematocrit 45%).
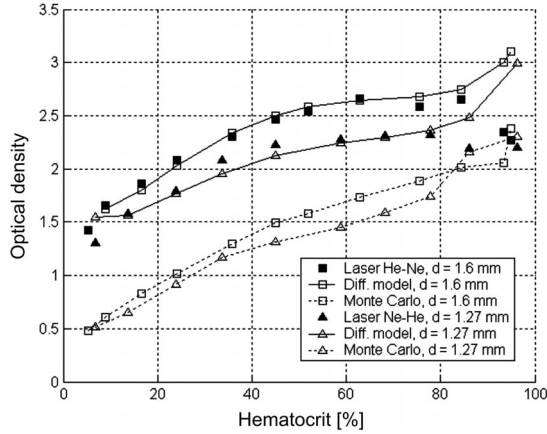
Fig. 8. Optical density as a function of hematocrit at He-Ne wavelength (632.8 nm). Measurement data *vs.* diffusion model and Monte Carlo simulation. Radius of source $a = 0.685$ mm, radius of detector $b = 1.0$ mm, at sample depth 1.27 and 1.6 mm. The whole blood is fully oxygenated.

the small divergence of light source, which is especially important for proper measurement of incident light beam.

Since the optical density predicted by the Monte Carlo simulation was lower than the measurement data, we have added off-sets to fit the model to the measurement outcomes. After adding the off-set, as shown in Fig. 9, the Monte Carlo model fits well the measured data for hematocrit up to 60–70%. Whereas, the diffusion model does not require off-sets in fitting the measured data. The accuracy of the Monte Carlo simulation referring to the measured data amounts to approx. 6%, and for the diffusion model up to 4%. In fact, the off-set in measurements indicates that the incident or
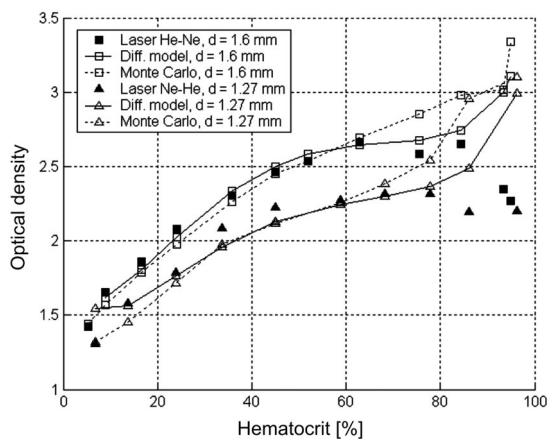
Fig. 9. Optical density as a function of hematocrit at He-Ne wavelength (632.8 nm) after adding off-set. Off-sets for MC: +0.96 for upper curve and +0.80 for lower curve. Rms error for upper curve 6.0% (MC), 4.4% (diff. model); lower curve: 4.9% (MC), 3.9% (diff. model).
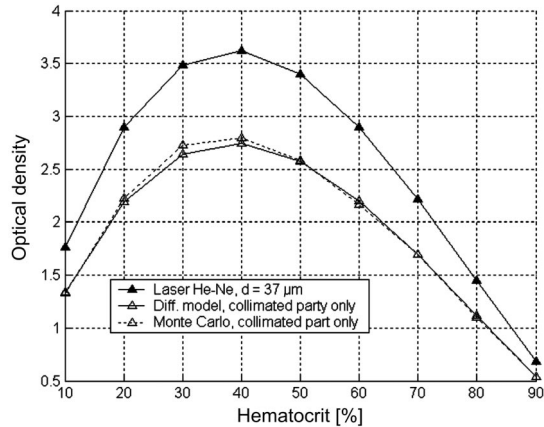
Fig. 10. Optical density as a function of hematocrit at He-Ne wavelength (632.8 nm), at very thin sample path (37 μm), collimated component only. The case of completely oxygenated whole blood.

detected light intensity could be under- or overestimated. Thus, the measurement data should be multiplied by a normalization factor to match it with the Monte Carlo predictions, which is a common technique [10]. A similar treatment was used during research of the adequacy of the Monte Carlo modeling in highly scattering phantom media with tissue. For the agreement with the Monte Carlo predictions, in all the cases the measured light flux had to be the required renormalization factor [10].

We decided to find the sources of discrepancy between models, comparing only the pure collimated component of Monte Carlo simulation and diffusion model with measured collimated part of light (see Fig. 10).

In fact, the agreement between the diffusion model and measurement data (see Fig. 8) was obtained by inserting the coefficient μ_s instead of the transport coefficient μ_s' in T_c expression, which caused significant deviation from the model. Thus, according to reference [2] the part of collimated light beam was responsible for the deviation from the diffusion model. The examination supposed to support these outcomes relied on the validation of T_c in diffusion model for a very thin whole blood sample (37 μm), so that the total detection of the light flux, which passed through the whole blood layer without any absorption and scattering events, would be possible [2]. However, Fig. 10 shows that the analytical expression of collimated transmittance T_c (see Eq. (9)) and its numerically simulated equivalent in the Monte Carlo model are almost the same, but both differ from the measurement results. As we can see in Fig. 10, the detector is not able to measure the pure collimated component of light, $i.e.$, the fraction of incident beam which was neither scattered nor absorbed in samples. Thus, distinguishing the collimated part of light from the diffuse background with the method used by Steinke and Shepherd, was not possible even when the detector was placed 2 m away from the sample. These results indicate that their measured values of collimated transmittance could be rather overestimated and, in fact, cannot be useful as complete explanation for discrepancy between the diffusion model and
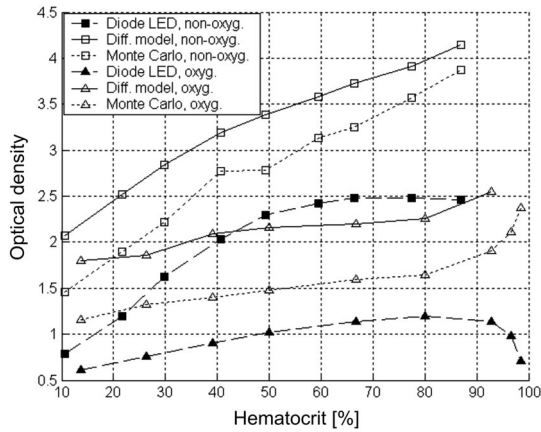
Fig. 11. Optical density of whole blood as a function of hematocrit at LED wavelength of 660 nm. Measurement data *vs.* diffusion model and Monte Carlo simulation. Radius of source a = 3.0, radius of detector b = 1.5 mm. The whole blood is fully oxygenated, sample path 1.27 and 1.6 mm.
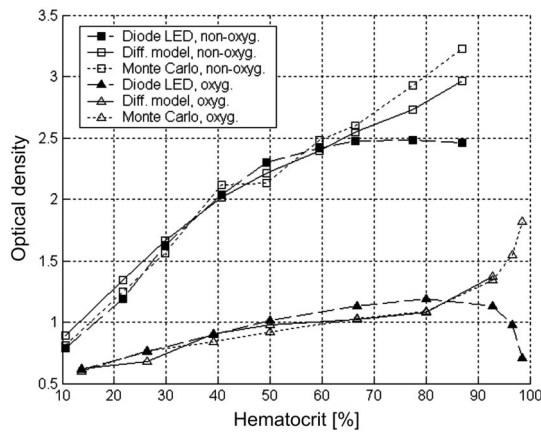
Fig. 12. Optical density of whole blood as a function of hematocrit at LED wavelength of 660 nm after considering off-sets. Off-sets for MC: –0.65 for upper curve, and –0.56 for lower, in diff. model of both –1 .18. Rms error for upper curve 4.9% (MC), 2.1% (diff. model); lower curve: 14.9% (MC), 2.1% (diff. model).

measurement data. Even though the alteration of T_c expression in the diffusion model was made, disagreement with measured data in relation to light sources with a larger divergence, such as diode LED, was still present (see Figs. 11 and 12).

We have compared the predictions of Monte Carlo and diffusion models to the optical density measurement for LED of 660 nm wavelength (Fig. 11). Steinke and Shepherd indicated that discrepancy between the diffusion model and the measurement data derives from the divergence of LED's beam and the small area of the detector in relation to the light source size. This was the reason for adding an off-set of 1.18 for

fitting measured data to the diffusion model (in fact, in Fig. 11 there are rough measurement data, without any off-set). Thus, adding an off-set to the measurement data practically corresponds to a multiplicative factor for intensity terms in the transmittance expression.
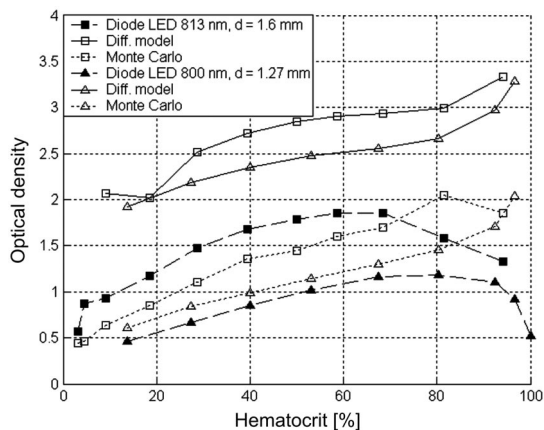
Fig. 13. Comparison of measurement data of optical density with diffusion and Monte Carlo simulation at LED's wavelengths of 800 and 813 nm. The case of fully oxygenated whole blood. At the wavelength of 800 nm: radius of source $a = 2.0$ mm, radius of detector $b = 1.5$ mm, and sample depth 1.6 mm; off-set for MC +0.38, diff.model –1.45. At the wavelength of 813 nm: radius of source $a = 2.0$ mm, radius of detector $b = 1.5$ mm, sample depth 1.27 mm; off-set for MC –0.18, diff.model –1.07. Rms error after correction, at 813 nm wavelength: 8.0% (MC), 5.1% (diff. model); at 800 nm wavelength: 13.7% (MC), 13.4% (diff. model).
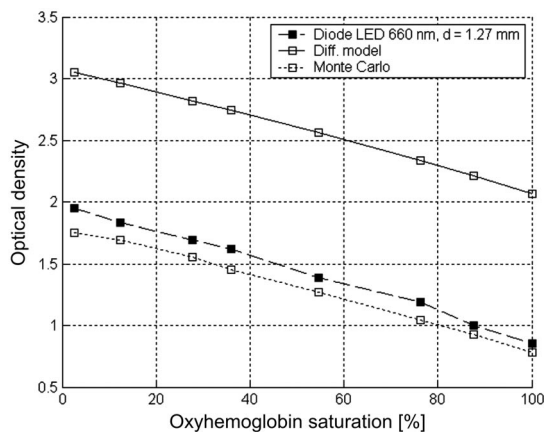
Fig. 14. Optical density as a function of oxyhemoglobin saturation for LED wavelength (660 nm). Measurement data *vs.* diffusion model and Monte Carlo model for LED (660 nm). Radius of source $a = 3.0$, radius of detector $b = 1.5$ mm. Sample depth 1.27 mm, hematocrit of whole blood is 36.5%. Offset for diffusion model –1.18, for Monte Carlo +0.1.

To fit the Monte Carlo simulation to measurement data, the off-set of –0.56 in the case of fully oxygenated whole blood was needed and for the non-oxygenated whole blood the off-set of –0.65. The Monte Carlo simulation fits the measurement data for hematocrit to values about 60–70% and its prediction of measurement data is almost the same as the diffusion model. With off-sets the accuracy of the Monte Carlo simulation comes up to 15% and for the diffusion model up to 2.0%. We have obtained the similar outcomes comparing the models with the optical density measurement for LED's wavelengths 800 and 813 nm (Fig. 13).

We inferred that the inaccuracy of diffusion model referring to measurement data could not only be due to the measurement problems of incident light beam. The predictions of Monte Carlo seem to confirm such observations, taking into consideration lower off-sets than the ones for diffusion model. Thus, the deviation from between the diffusion model can be explained also by its failure caused by the increase of anisotropic radiance in the thin sample of whole blood, whereas the measurement problem connected with the divergence of beam or perturbation of light flux, in fact, can be described by off-sets coming from the Monte Carlo simulation.

The Monte Carlo predictions have also more advantage over diffusion model in fitting the dependence of oxyhemoglobin saturation at the LED wavelength of 660 nm, as shown in Fig. 14. To fit the measurement data, the Monte Carlo simulation requires the off-set of +0.1, while in the diffusion model the off-set amounts to –1.18. The conformity of Monte Carlo simulation with the measurement data is almost the same, as in the diffusion theory. After adding the off-sets, the accuracy of Monte Carlo simulation was about 0.7%, whereas for the diffusion model 0.6%.

7. Conclusions

The subject of this work was the modeling of transmittance measurement in the whole blood medium. We have developed Monte Carlo simulation using the assumption for approximation of photon transport in highly scattering media. It was assumed that transmittance in the model depends on the technique of mean free path length simulation in a given direction and location of photon. The Monte Carlo simulation was compared with the diffusion model in the cuvette measurement conditions, with the sample depth insignificantly different from the effective free path length. Although, the simulations revealed that curves of the optical density predicted by the Monte Carlo simulation and the diffusion model keep a similar shape, there is an off-set between them. The discrepancy between the models was caused by the failure of diffusion model due to the anisotropic radiance, producing deviation in the linear anisotropy assumed in deriving the diffusion equation. Such observations were confirmed during the comparison of models and measurement data. Thus, the lower off-sets of Monte Carlo simulation revealed the weakness of the diffusion model at low values of albedo, and strong forward scattering. In fact, the Monte Carlo simulation gives insight into measurement problem such as the perturbation of light flux, the

divergence of light beam or the residual anisotropy of the detector response. Moreover, the research showed that after adding off-sets Monte Carlo predictions agree with measurement data for hematocrit up to 60–70%. Fortunately, such validity of our model is completely satisfactory, because in most biomedical applications hematocrit will remain at level lower than 60%.

References

[1] Reynolds L., Johnson C., Ishimaru A., *Diffuse reflectance from a finite blood medium: applications to the modeling of fiber catheters*, Applied Optics **15**(9), 1976, pp. 2059–67.

[2] Steinke J.M., Shepherd A.P., *Diffusion model of the optical absorbance of whole blood*, Journal of the Optical Society of America A: Optics, Image Science and Vision **5**(6), 1988, pp. 813–22.

[3] Szczepanowski R., *Multiple light scattering model in blood medium using Monte Carlo method*, Ph.D. Thesis, Wrocław University of Technology, Poland 2002 (in Polish).

[4] Tversky V., *Absorption and multiple scattering by biological suspensions*, Journal of the Optical Society of America **60**(8), 1970, pp. 1084–93.

[5] Lipowsky H.H., Usami S., Chien S., Pittman R.N., *Hematocrit determination in small bowel bore tubes from optical density measurements under white light illumination*, Microvascular Research **20**(1), 1980, pp. 51–70.

[6] Flock S.T., Patterson M.S., Wilson B.C., Wyman D.R., *Monte Carlo modeling of light propagation in highly scattering tissues – I: Model prediction and comparison with diffusion theory*, IEEE Transactions on Biomedical Engineering **36**(12), 1989, pp. 1162–7.

[7] Flock S.T., Wilson B.C., Patterson M.S., *Hybrid Monte Carlo-diffusion theory modelling of light distributions in tissue*, SPIE **908**, 1988, pp. 20–8.

[8] van Gemert M.J.C, Jacques S.L., Sterenborg H.J.C.M., Star W.M., *Skin optics*, IEEE Transactions on Biomedical Engineering **36**(12), 1989, pp. 1146–54.

[9] Wilson B.C., *A Monte Carlo model for the absorption and flux distributions of light in tissue*, Medical Physics **10**(6), 1983, pp. 824–30.

[10] Flock S.T., Wilson B.C., Patterson M.S., *Monte Carlo modeling of light propagation in highly scattering tissues – II: Comparison with measurements in phantoms*, IEEE Transactions on Biomedical Engineering **36**(12), 1989, pp. 1169–73.

[11] Song Z., Dong K., Hu X.H., Lu J.Q., *Monte Carlo simulation of converging laser beams propagating in biological materials*, Applied Optics **38**(13), 1999, pp. 2944–9.

[12] Roggan A., Drorschel K., Minet O., Wolff D., Muller G., *The optical properties of biological tissue in the near infrared wavelength range-review and measurements*, [In] *Laser-Induced Interstitial Thermotheraphy*, G. Muller, A. Roggan [Eds.], SPIE Press, LMZ GmbH, Berlin, pp. 10–44.

[13] Hahn A., *Optimization of laser measuring methods for their use in extracorporeal circulation*, Ph.D. Thesis, Wroclaw University of Technology, Poland 1996.

[14] Czerwinski M., Mroczka J., *New concept of hybrid method to describe the light transmittance in terms of multiple light scattering – monodisperse distribution approximation*, Optica Applicata **31**(4),2001, pp. 719–29.

[15] Mishchenko M.I., Hovenier J.W., Travis L.D., *Light Scattering by Nonspherical Particles: Theory, Measurements, and Applications*, Academic Press, San Diego 2000.

[16] Hemenger R.P., *Optical properties of turbid media with specularly reflecting boundaries: application to biological problems*, Applied Optics **16**(7), 1977, pp. 2007–12.

[17] Zdrojkowski R.J., Pisharothy N.R., *Optical transmission and reflection by blood*, IEEE Transactions on Biomedical Engineering **17**(2), 1970, pp. 122–8.

[18] Marchuk G.I., Mikhailov G.A., Nazaraliev M.A., Dabinjan R.A., Kargin B.A., *The Monte Carlo Methods in Atmospheric Optics*, Springer-Verlag, New York 1980.

[19] PRAHL S.A., KAEIJZER M., JACQUES S.L., WELCH A.J., *A Monte Carlo model of light propagation in tissue*, SPIE Institute Series Vol. 5, 1989, pp. 102–10.

[20] PRAHL S.A., *Light transport in tissue*, Ph.D. Thesis, University of Texas at Austin, 1980.

[21] WANG L.H., JACQUES S.L., ZHENG L.Q., *MCML – Monte Carlo modeling of light transport in multi-layered tissues*, Computer Methods and Programs in Biomedicine **47**(2), 1995, pp. 131–46.

[22] TYCKO D.H., METZ M.H., EPSTEIN E.A., GRINBAUM A., *Flow–cytometric light scattering measurements of red blood cell volume and hemoglobin concentration*, Applied Optics **24**(9), 1985, pp. 1355–65.

[23] SZCZEPANOWSKI R., GUSZKOWSKI T., MROCZKA J., *Influence of osmotic pressure on light scattering by red blood cells*, IMEKO XVI Congress Wien, vol.VII, Topic 13, 2000, pp. 119–24.

[24] MOHANDAS N., CLARK M.R., JACOBS M.S., SHOHET S.B., *Analysis of factor regulating erythrocyte deformability*, Journal of Clinical Investigation **66**(3), 1980, pp. 563–73.

[25] GANONG W., *Review of Medical Physiology*, Chap. 6–27, Appleton and Lang, Norwalk 1991.

[26] MROCZKA J., WYSOCZANSKI D., ONOFRI F., *Optical parameters and scattering properties of red blood cells*, Optica Applicata **32**(4), 2002, pp. 691–700.

[27] MISHCHENKO M.I., TRAVIS L.D., *Capabilities and limitations of a current Fortran implementation of the T-matrix method for randomly orientated, rotationally symmetric scatteres*, Journal of Quantitative Spectroscopy and Radiative Transfer **60**(3), 1998, pp. 309–24.

[28] SCHMITT J.M., MIHM F.G., MEINDL J.D., *New methods for whole blood oximetry*, Annals of Biomedical Engineering **14**(1), 1986, pp. 35–52.

[29] SCHMITT J.M., XIONG Z.G., MILLER J., *Measurement of blood hematocrit by dual-wavelength near-IR photoplethysmography*, Proceedings of SPIE **1641**, 1992, pp. 150–61.